ISSN : 0974 - 7486 Volume 10 Issue 11

Materials Science

An Indian Journal

Full Paper

MSAIJ, 10(11), 2014 [454-460]

Growth, characterization and computational analysis on the NLO crystal 3-pyridinecarboxamide

N.Sakthivel[1], L.Arivuselvam[1], K.Suguna[1], K.Subramani[2], V.Aroulmoji[3], P.M.Anbarasan[1,4]*

[1]Department of Physics, Periyar University, Salem - 636 011, Tamil Nadu, (INDIA)

[2]Department of Chemistry, K.M.C.P.G.S., Lawspet, Puducherry – 605008, (INDIA)

[3]Mahendra Educational Institutions, Mallasamudram - 637 503, Tamil Nadu, (INDIA)

[4]Centre for Nanoscience & Nanotechnology, Periyar University, Salem - 636 011, Tamil Nadu, (INDIA)

E-mail : anbarasanpm@gmail.com

ABSTRACT

The growth and characterization of a new nonlinear organic crystal, 3-pyridinecarboxamide (3PCA) is reported. The growth of single crystals of 3PCA was accomplished by the slow evaporation solution growth method. The X-ray diffraction analysis confirms the crystal structure. The Kurtz powder second harmonic generation (SHG) test showed potential for optical SHG. The UV cut-off transmission was identified from the UV–Vis absorption spectra. The mechanical response of the crystal has been studied using Vickers microhardness technique. The elastic stiffness constant (C_{11}) were calculated for different loads using Wooster's empirical formula. The gap between highest occupied molecular orbital and the lowest unoccupied molecular orbital is calculated, which is useful for estimating the efficiency of second harmonic generation.

KEYWORDS

Crystal growth;
DFT calculation;
HOMO;
LUMO;
UV-Vis studies;
Hardness studies.

INTRODUCTION

Nonlinear optics is concerned with the interaction of electromagnetic fields with various media to produce new electromagnetic fields altered in phase, frequency or amplitude from the incident fields. The investigations on materials with potential for large second-order nonlinear optical (SONLO) applications are very much emphasized in view of the key-role played by them in the frequency conversion process required for the production of new laser output covering ultraviolet and blue-green region. Recently extensive research is going on materials with the capable of efficient frequency conversion of infrared (IR) radiation to visible and ultraviolet (UV) wavelengths. Especially, those materials, which can generate highly efficient second harmonic blue light using laser diodes, are of great interest for applications including optical computing, optical information processing, optical disk data storage, medical diagnostics, etc. Materials with large nonlinear coefficients, and appropriate refractive index (or birefringence) for phase matching, very low absorption, good optical quality, hardness and ability to take high polish, low two photon absorption coefficient and high laser damage threshold are needed in order to realize many of these applications[1,2]. In the recent past, extensive investigations are being carried out on organic NLO[3-6] materials due to their high SHG efficiency, synthetic flexibility and

better laser damage threshold compared with inorganic materials. The origin of nonlinearity in these materials is due to the presence of delocalized electron systems connecting donor and acceptor groups, which enhance their asymmetric polarizability. This report is focused on the growth of crystals of 3-pyridinecarboxamide (3PCA) and also to study the mechanical response of the crystal using Vickers microhardness technique. The elastic stiffness constant (C_{11}) were calculated for different loads using Wooster's empirical formula. The gap between highest occupied molecular orbital and the lowest unoccupied molecular orbital is calculated, which is useful for estimating the efficiency of second harmonic generation.

SOLUBILITY STUDIES

The commercially available 3-pyridinecarboxamide (3PCA) ($C_6H_6N_2O$) was further purified by repeated recrystallization process. In order to obtain single crystals of high quality, purification of starting material was found to be an important step. The recrystallized salt was the charge material for the growth of 3PCA. To grow bulk crystals from solution by slow evaporation technique, it is desirable to select a solvent in which it is moderately soluble. The size of a crystal depends on the amount of material available in the solution, which in turn is decided by the solubility of the material in that solvent. Hence, we have determined the solubility as deionized water[7]. Solubility in deionized water was found good and the crystals grown were found to have better shape and transparency. Good transparent single crystals were obtained after a week. Figure 1 shows the grown crystal of 3PCA at different solvents (a) deionised water (b) alcohol (c) ethylene and (d) meth-

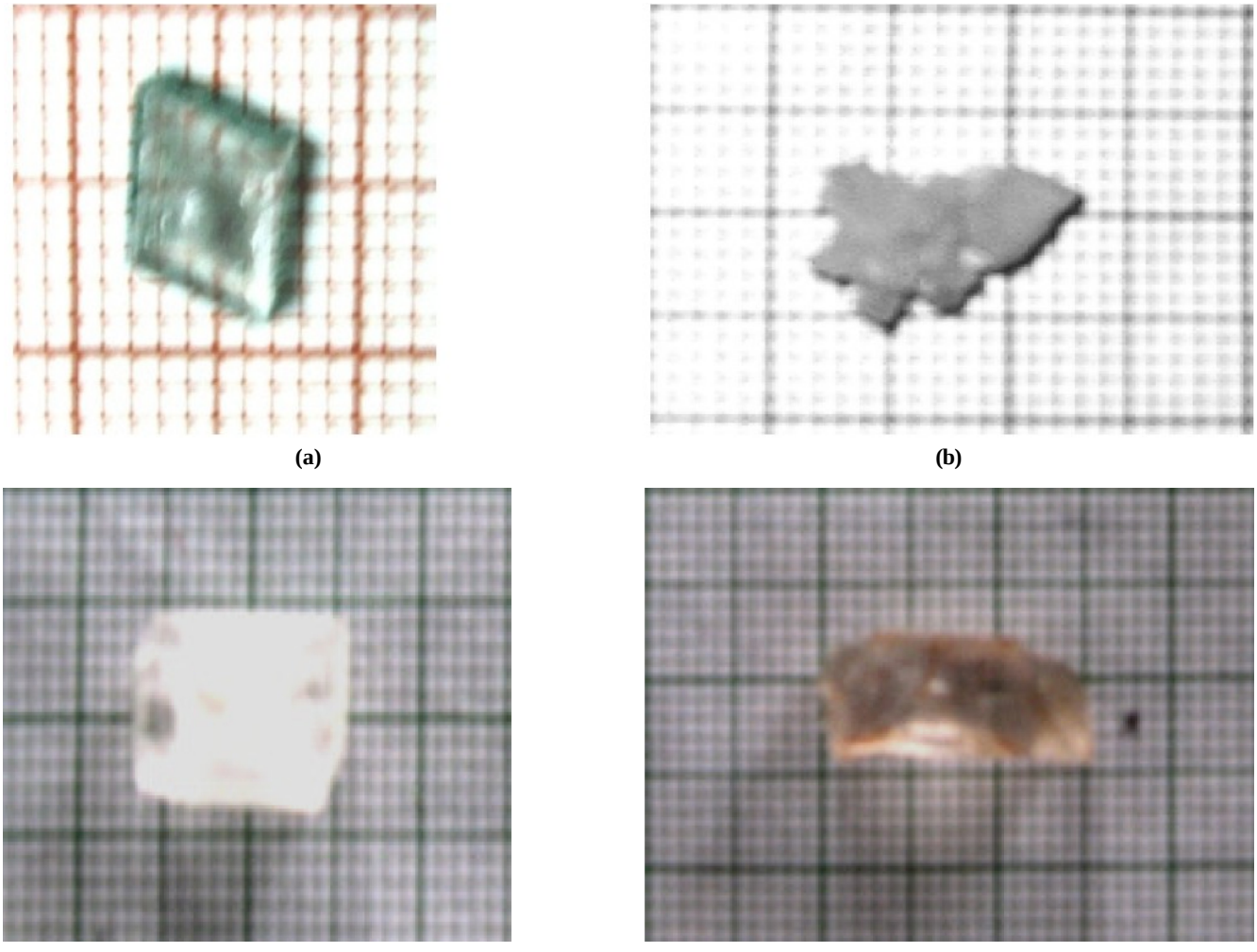

Figure 1 : Grown crystal of 3PCA with different solvents (a) deionised water (b) alcohol (c) ethylene and (d) methylene.

ylene with an optimized solution pH value of 3.5.

POWDER X-RAY DIFFRACTION ANALYSIS

The XRD data the crystal still possesses monoclinic symmetry with the space group $P2_1/_C$, a well-known centrosymmetric space group thus satisfying the requirements for second-order NLO activity. The lattice parameter values of the crystal have been calculated using least-squares fit method and they are found to be *a* = 3.931Å, *b* = 15.607Å, *c* =9.472Å, α=γ=90°, β=98.63° respectively as given in the TABLE 1. The crystallographic data obtained in the present study were found to be in good agreement with the data reported in literature[8]. The chemical structure of 3PCA was depicted in Figure 2.

TABLE 1 : Crystallographic data of 3PCA

Crystal data	Parameters
Formula	$C_6H_6N_2O$
Weight	122.13
Crystal system	Monoclinic
Space group	P21/c
a	3.931Å
b	15.607 Å
c	9.472 Å
α=γ	90°
β	98.63°
*D*x	1.122 g/cm^3
V	560.8 Å^3
Z	4
D_x	1.4463 g/cm^{-3}
D_m	1.398 g/cm^{-3}
Colour	Colorless

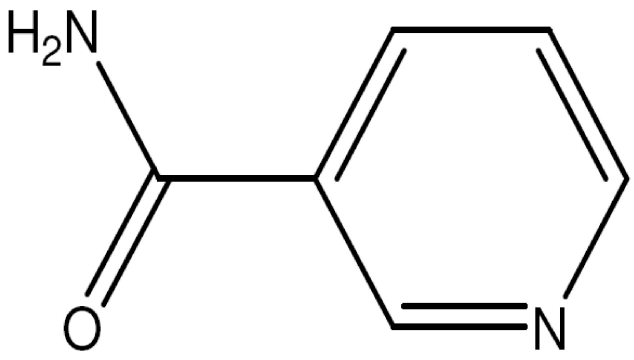

Figure 2 : Chemical structure of 3PCA

OPTICAL STUDIES

The optical transmittance spectrum of 2mm thickness polished 3PCA crystal was recorded using Perkin Elmer Lamda 35 spectrophotometer and is shown in Figure 3. Normally aromatic compound absorbs light in UV region and the highly conjugated aromatic molecules absorb light in the visible region. The lower cutoff wavelength is found at 220 nm. This is assigned to n to π* transition and it may be attributed to the excitation of charge from the aromatic ring also this transition gives white colour to the grown crystal. High transmittance is observed at the Nd: a YAG laser fundamental and second harmonic wavelength which indicates that the grown crystal is well suited for frequency conversion of 1064 nm laser radiation. The optical transparency characteristic of the grown crystal is an attractive for opto-electronic applications[9] since these compounds do not absorb radiation in the visible region of the electronic spectrum. An absorption peak observed at 190 nm is due to the presence of amide group π– π* transition.

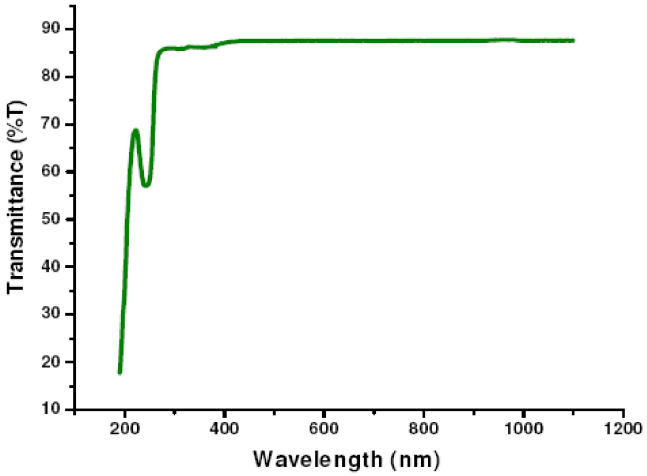

Figure 3 : UV–Vis spectrum of 3PCA

ENERGY BAND GAP

The variation of $(\alpha h\nu)^2$ versus incident photon energy (hυ) using the Tauc[10] relation in the fundamental absorption region was plotted and is shown in Figure 4. The optical band gap energy (E_g) was estimated by extrapolation of the linear portion of the curve to a point $(\alpha h\upsilon)^2 = 0$. Using this method, the optical energy band gap of the crystal is found as 5.8 eV. This high value of

band gap energy and the lower cut-off wavelength of the crystal assert the suitability of the crystal for photonic and optical applications[11].

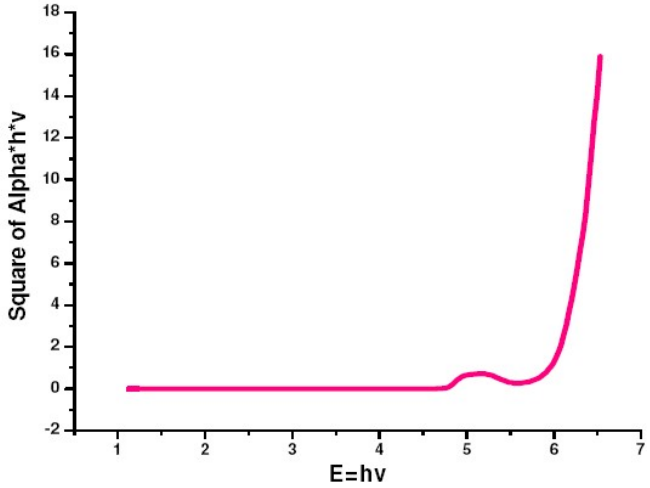

Figure 4 : The variation of $(\alpha hv)^2$ and incident photon energy (hv) of 3PCA

MICRO HARDNESS STUDIES

Micro hardness measurements[12-14] were carried out using Leitz Weitzler hardness tester fitted with a diamond indentor. All the indentation measurements were carried out on the freshly cleaved samples. The indentation was made by varying the load from 25 to 200 gm and the time of indentation was kept at 5 sec. The indented impressions were approximately square. The crystal surfaces were indented at different sites. Diagonal lengths of the indented impression were measured using calibrated micrometer attached to the eyepiece of the microscope. Several indentations were made on each sample. The average value of the diagonal lengths of indentation mark was used to calculate the hardness. The Microhardness is calculated using the expression, $H_v = 1.8544P/d^2$ Kg mm^{-2}, where, P is the applied load in Kg and d the average diagonal length of the Vickers impression in mm after unloading. It is observed that the increase in hardness with applied load. Although hardness has been defined in several ways, it is now generally accepted that it is the resistance offered to dislocation motion. There are several contributions to the resistance to the dislocation motion and they can be classified into two types (i) the intrinsic resistance which depends on some structure insensitive physical parameter of the crystal and (ii) a disorder parameter which depends on the concentration of the imperfections.

The non-liner variation of microhardness is due to the presence of imperfections. These imperfections can be vacancies, impurity-vacancy pairs, dislocations, low angle grain boundaries etc. The plot of hardness (H_v) versus load for the title crystal is shown in Figure 5.

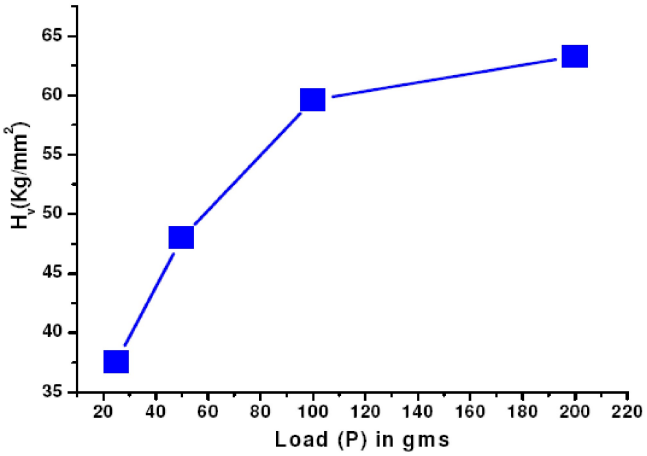

Figure 5 : Plot of H_v versus load of 3PCA

ELASTIC STIFFNESS CONSTANT

The elastic stiffness constant (C_{11}) was calculated for different loads using Wooster's empirical formula[14] $C_{11} = H_v^{7/4}$. The C_{11} values are shown in TABLE. 2. This value gives an idea about the tightness of bonding between neighboring atoms. The high value shows that the binding forces between the atoms were quite strong. It was calculated for the loads from 25gm to 200gm. The Plot of H_v versus Elastic Stiffness Constant for the title crystal is shown in Figure 6.

TABLE 2 : Elastic stiffness constant

Load (g)	C_{11} (10^{14}Pa)
25	9.8116
50	1.5043
100	21.9706
200	24.4128

KURTZ POWDER SHG TEST

A Q-switched Nd: YAG laser beam of wavelength 1064 nm with an input power of 2.5 mJ and pulse width

Full Paper

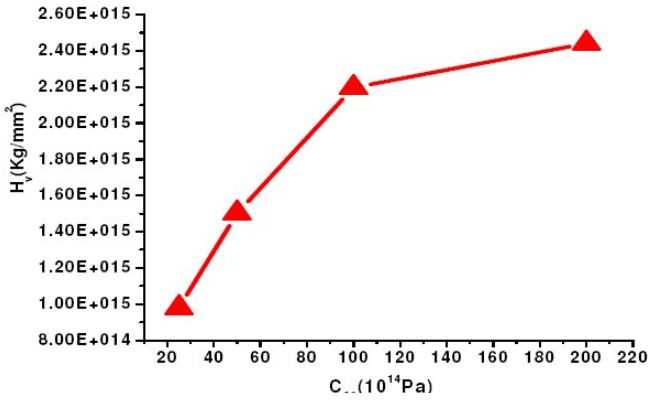

Figure 6 : Plot of H_v versus load of elastic stiffness constant

8 ns with a repetition rate of 10 Hz is used to illuminating the powdered sample. The grown crystal is powdered with a uniform particle size of 125–150 μm, and then packed in a microcapillary of uniform bore and exposed to the laser radiation[15,16]. The SHG conversion efficiency is found to be 3 times greater value of the KDP (9 mV). This increased value may be due to the presence of amide in the grown material.

HYPERPOLARIZABILITY CALCULATION

For calculating the hyperpolarizability, the geometry of the investigated compound is treated as an isolated molecule. The optimization has been carried out using DFT(6-31++G(d,p)) Method. The geometries are fully optimized without any constraint with the help of analytical gradient procedure implemented within Gaussain98W program[18]. The electric dipole moment and dispersion free first-order hyperpolarizability are calculated using finite field method. The finite field method offers a straight forward approach to the calculation of hyperpolarizability. The 3-21(d,p) basis set gives remarkably good geometries for such a small basis set and in fact it is used for the geometry optimization of some high accuracy energy methods.

The nonlinear properties of an isolated molecule in an electric field $E_i(\omega)$ can be represented by the Taylor expansion of the total dipole moment mi induced by the field

Taken at zero field,

Dipole moment $\mu_i = -\left[\frac{\partial^2 E}{\partial F_i \partial F_j}\right]_0$

Components of polarizability tensor: $\alpha_{ij} = -\left[\frac{\partial E}{\partial F_i}\right]_0$

Components of hyperpolarizability tensor: $\beta_{ijk} = -\left[\frac{\partial^3 E}{\partial F_i \partial F_j \partial F_k}\right]_0$

These components are to be distorted by an external electric field. The value of total static polarizability and hyperpolarizability are obtained from the following equation,

$$\beta_{tot} = [(\beta_{xxx} + \beta_{xyy} + \beta_{xzz})^2 + (\beta_{yyy} + \beta_{yzz} + \beta_{yxx})^2 + (\beta_{zzz} + \beta_{zxx} + \beta_{zyy})^2]^{1/2}$$

In the presence of an applied electric field, first order hyperpolarizability is a third rank tensor that can be described by a 3×3×3 matrix. The components of the 3D matrix can be reduced to 10 components because of the Kleinman symmetry[19]. The matrix can be given in the lower tetrahedral format. It is obvious that the lower part of the 3×3×3 matrix is a tetrahedral. The calculation of NLO properties with high accuracy is challenging and requires consideration of many different issues. Computational techniques are becoming valuable in designing, modeling and screening novel NLO materials. The calculated value of hyperpolarizability for the title compound is 0.818586×10^{-30} esu, which is nearly 4 times that of urea (0.20920×10^{-30} esu). This highest value of hyperpolarizability may be due to the presence of electro-negative nitro group and π bonds. The calculated values of dipole moment and hyperpolarizability values are tabulated in TABLE 3. The β_{zzz} direction shows biggest value of hyperpolarizability which insists that the delocalization of electron cloud is more that direction than other directions. The NLO responses can be understood by examining the energetic of frontier molecular orbitals. Figure 7a and Figure 7b shows the highest occupied molecule orbital (HOMO) and lowest unoccupied molecule orbital (LUMO) of 3PCA. There is an inverse relationship between hyperpolarizability and HOMO–LUMO.

HOMO energy =-0.298 a.u
LUMO energy = 0.208 a.u
HOMO–LUMO energy gap = 0.506 a.u

The Representation of the orbital involved in the

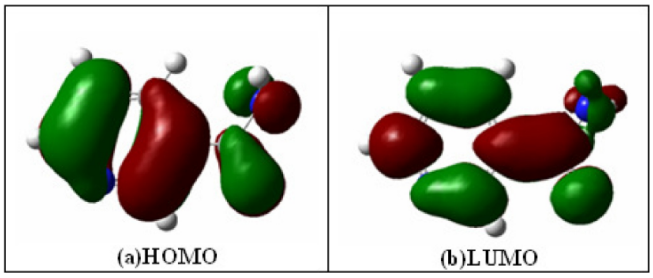

Figure 7 : HOMO and LUMO representation of 3PCA

TABLE 3 : The dipole moment (μ) and first-order hyperpolarizibility (β) of 3PCA derived from DFT calculation

β_{xxx}	0.204492
β_{xxy}	0.0565447
β_{xyy}	-0.013891
β_{yyy}	-0.0026034
β_{zxx}	-0.75063
β_{xyz}	0.105752
β_{zyy}	-0.17586
β_{xzz}	-0.21523
β_{yzz}	0.0221795
β_{zzz}	0.111822
β_{tot}	0.818586
μ_x	1.491223686
μ_y	0.0000627771
μ_z	2.227837147
μ	1.928502945

electronic transition for (a) HOMO-4 (b) LUMO+1 (c) LUMO+14 (d) HOMO-0 (e) HOMO-2 (f) LUMO+4 (g) HOMO-3 (h) HOMO-1 (i) LUMO+16

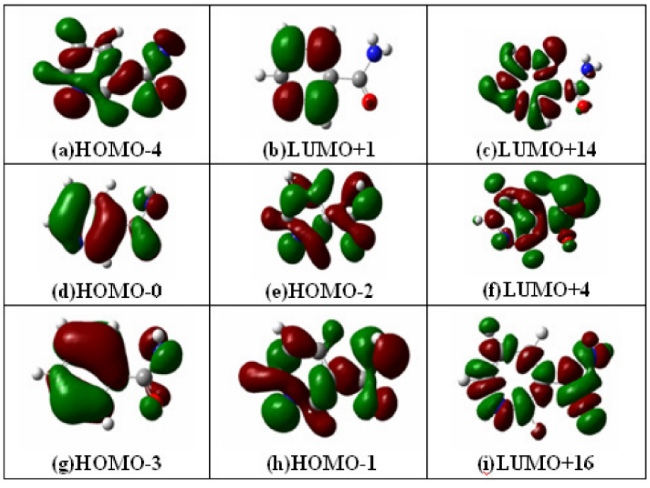

Figure 8 : Representation of the orbital involved in the electronic transition for HOMO-4 (b) LUMO+1 (c) LUMO+14 (d) HOMO-0 (e) HOMO-2 (f) LUMO+4 (g) HOMO-3 (h) HOMO-1 (i) LUMO+16

are shown in the Figure 8.

ELECTRONIC EXCITATION MECHANISM

The static polarizability value[20,21] is proportional to the optical intensity and inversely proportional to the cube of transition energy. With this concept, larger oscillator strength (f_n) and $\Delta\mu_{gn}$ with lower transition energy (E_{gn}) is favourable to obtain large first static polarizability values. Electronic excitation energies, oscillator strength and nature of the respective excited states were calculated by the closed-shell singlet calculation method and are summarized in TABLE 4.

TABLE 4 : Computed absorption wavelength (λ_{ng}), energy (E_{ng}), oscillator strength (f_n) and its major contribution.

n	λ_{ng}	E_{ng}	f_n	Major contribution
1	228.2	5.43	0.0009	H-4->L+1(30%) H-3->L+1(21%) H-4->L+14(9%) H-4->L+19(5%)
2	199.4	6.22	0.1948	H-0->L+1(71%) H-1->L+4(10%)
3	197.6	6.27	0.0147	H-2->L+4(32%) H-2->L+1(11%) H-3->L+4(11%) H-2->L+16(6%)

(Assignment; H=HOMO, L=LUMO, L+1=LUMO+1, etc.)

CONCLUSION

Good quality crystals of 3-pyridinecarboxamide (3PCA) were grown from aqueous solution by slow evaporation technique at room temperature. The optical transmittance window, lower cut off wavelength, band gap of the title crystal has been identified by UV-VIS-NIR studies. The results of the response of the mechanical behaviour of the crystal will have significant effect on machining the crystal for device purpose. Density functional theory calculations were performed for the title nonlinear optical crystal to evaluate the first order hyperpolarizability value. The calculated value of hyperpolarizability for the title compound is 0.818586×10^{-30} esu, which is nearly 4 times that of urea (0.20920×10^{-30} esu). This could be a new series of

prospective crystals for second-order NLO applications such as electro optic or frequency doubler of conventional diode lasers.

REFERENCES

[1] D.S.Chemla, J.Zyss, (Eds); Nonlinear Optical Properties of Organic Molecules and Crystals, Academic Press, New York, **(1987)**.

[2] P.N.Prasad, D.J.Williams; Introduction to Nonlinear Optical Effects in Molecules and Polymers, Wiley-Interscience, New York, **(1991)**.

[3] S.Chenthamarai, D.Jayaraman, P.M.Ushasree, K.Meera, C.Subramanian, P.Ramasamy; Mater.Chem.Phys., **64**, 179 **(2000)**.

[4] M.Kitazawa, R.Higuchi, M.Takahashi; Appl.Phys.Lett., **64**, 2477 **(1994)**.

[5] L.Misoguti, A.T.Varela, F.D.Nunes, V.S.Bagnato, F.E.A.Melo, J.Mendes Filho, C.Zilio; Opt.Mater., **6**, 147 **(1996)**.

[6] W.S.Wang, M.D.Aggarwal, J.Choi, T.Gebre, A.D.Shields, B.G.Penn, D.O.Frazier; J.Crystal Growth, **198,199**, 578 **(1999)**.

[7] Vincent Aroulmoji, Mohamed Mathlouthi, M.O.Portmann-Richardson; Solution Properties and the Masking of Unpleasant Tastes of Nicotine – Sweetener - Water Mixtures, IJPSR, **4(6)**, 2190-2198 **(2013)**.

[8] Yoshihisa Miwa, Takashi Mizuno, Kazunori Tsuchida, Tooru Taga, Yutaka Iwata; Acta Cryst., **B55**, 78-84 **(1999)**.

[9] K.Krishna Rao, V.Surender, B.Savitharani; Bull Mater.Sci., **25**, 641–6 **(2002)**.

[10] S.Sirohi, T.P.Sharma; Optical Mater., **13**, 267 **(1999)**.

[11] N.Vijayan, G.Bhagavannarayana, G.C.Budakoti, B.Kumar, V.Upadhyaya, S.Das; Mater.Lett., **62**, 1252 **(2008)**.

[12] B.W.Mott; Micro Indentation Hardness Testing, Butter Worths, London, 206 **(1956)**.

[13] Meyer; Some aspects of the hardness of metals, Ph.D.Thesis, Dreft, **(1951)**.

[14] E.M.Onitsch; Mikroskopie, **2**, 131 **(1947)**.

[15] W.A.Wooster; Rep.Phys.Phys., **16**, 62–82 **(1953)**.

[16] S.K.Kurtz, T.T.Perry; J.Appl.Phys., **39(8)**, 3798 **(1968)**.

[17] S.K.Kurtz; J.Quantum Electron, **4**, 578 **(1968)**.

[18] M.J.Frish, G.W.Trucks, H.B.Schlegel, G.E.Schlegel, G.E.Scuseria, M.A.Robb, J.R.Cheeseman, V.G.Zakrzewski, J.A.Montgomery Jr., R.E.Stratmann, J.C.Burant, S.Dapprich, J.M.Millam, A.D.Daniels, K.N.Kudin, M.C.Strain, O.Farkas, J.Tomasi, V.Barone, M.Cossi, R.Cammi, B.Mennucci, C.Pomelli, C.Adamo, S.Clifford, J.Ochterski, G.A.Petersson, P.Y.Ayala, Q.Cui, K.Morokuma, D.K.Malick, A.D.Rabuck, K.Raghavachari, J.B.Foresman, J.Cioslowski, J.V.Qrtiz, A.G.Baboul, B.B.Stefanov, G.Liu, A.Nanayakkara, C.Gonzalez, M.Challacombe, P.M.W.Gill, B.Johnson, W.Chen, M.W.Wong, J.L.Andres, C.Gonzalez, M.Head-Gordon, E.S.Replogle, J.A.Pople; GAUSSIAN 98, Revision A.7, Gaussian Inc., Pittsburg, PA, **(1998)**.

[19] D.A.Kleinman; Phys.Rev., **126** 1977 **(1962)**.

[20] K.Wu, C.Liu, C.Mang; Opt.Mater., **29**, 1129–1137 **(2007)**.

[21] S.Iran, W.M.F.Fabian; Dyes Pigments, **70**, 91–96 **(2006)**.